Partitioning of microbially respired CO_2 between indigenous and exogenous carbon sources during biochar degradation using radiocarbon and stable carbon isotopes

Niels C. Munksgaard[a, b], Anna V. McBeath[a, c], Philippa L. Ascough[d], Vladimir A. Levchenko[e], Alan Williams[e], Michael I. Bird[a, f]

[a] College of Science and Engineering and Centre for Tropical Environmental and Sustainability Science, James Cook University, Smithfield, QLD 4878, Australia

[b] Research Institute for the Environment and Livelihoods, Charles Darwin University, Casuarina, NT 0810, Australia

[c] Department of Agriculture and Fisheries, Queensland Government, South Johnstone, QLD 4859, Australia

[d] NERC Radiocarbon Facility, Scottish Universities Environmental Research Centre (SUERC), Scottish Enterprise Technology Park, Rankine Avenue, East Kilbride G75 0QF, UK

[e] Australian Nuclear Science and Technology Organisation (ANSTO), Kirrawee DC, NSW 2232, Australia

[f] ARC Centre for Excellence for Australian Biodiversity and Heritage, James Cook University, Smithfield, QLD 4878, Australia

Abstract

Pyrolised carbon in biochar can sequester atmospheric CO_2 into soil to reduce impacts of anthropogenic CO_2 emissions. When estimating the stability of biochar, degradation of biochar carbon, mobility of degradation products and ingress of carbon from other sources must all be considered. In a previous study we tracked degradation in biochars produced from radiocarbon-free wood and subjected to different physico-chemical treatments over three years in a rainforest soil. Following completion of the field trial, we report here a series of in-vitro incubations of the degraded biochars to determine CO_2 efflux rates, ^{14}C concentration and $\delta^{13}C$ values in CO_2 to quantify the contributions of biochar carbon and other sources of carbon to the CO_2 efflux. The ^{14}C concentration in CO_2 showed that microbial degradation led to respiration of CO_2 sourced from biochar carbon (≈ 0.5 - 1.4 µmoles CO_2 / g biochar C / day) along with a component of carbon closely associated with the biochars but derived from the local environment. Correlations between ^{14}C

concentration, $\delta^{13}C$ values and Ca abundance indicated that Ca^{2+} availability was an important determinant of the loss of biochar carbon.

Key Words

Biochar, ^{13}C, ^{14}C, Respiration, Degradation, Immobilisation

Introduction

Biochar is pyrolyzed carbon (PyC) derived from the incomplete combustion of biomass. When incorporated into soil, biochar has the potential to provide long-term carbon sequestration that is potentially able to offset a significant fraction of anthropogenic emissions (Woolf et al. 2010, Wang et al. 2014). However, biochar includes a range of carbon compounds with variable degrees of resistance to degradation (Bird et al. 1999; Kanaly and Harayama 2000; Hammes et al. 2008; Bird et al. 2015).

The degree to which biochar is susceptible to degradation is controlled by the temperature of pyrolysis, the nature of the material pyrolized and environmental conditions that influence the activity of microbial communities and organo-mineral interactions during degradation (e.g. soil type, temperature, moisture, pH and Ca^{2+} availability (Pietikainen et al. 2000; Hockaday et al. 2007; Whittinghill and Hobbie 2012; Bird et al. 2017). Recent research has mostly emphasised the role of microbial degradation of biochar (e.g. Forbes et al. 2006; Fang et al. 2014; Kuzyakov et al. 2014; Tilston et al. 2016) and these studies have directly demonstrated respiration of PyC using both $^{13}C/^{12}C$ and radiocarbon (^{14}C) as tracers of PyC conversion into CO_2, microbial biomass, and soil organic carbon. In contrast, a year-long in-vitro experiment by Zimmerman (2010) found abiotic CO_2 production rates equivalent to those of microbial oxidation in several types of biochars.

Recently Bird et al (2017) examined the controls on the degradation of biochars produced at different temperatures from radiocarbon-free wood by subjecting them to different physico-chemical treatments over three years in a humid tropical rainforest soil in NE Australia. Mass balance calculations and measurements of ^{14}C concentration in the biochars demonstrated a strong relationship between degradation and loss of indigenous (biochar) carbon, with carbon losses offset to various degrees by the simultaneous addition of exogenous (leaf litter derived) carbon from the local environment. High net carbon loss in biochars pyrolised at 300^{o}C implied a relatively rapid total degradation of the material to gaseous or solubilized forms over a few decades. Substantially lower

net losses of C in biochar pyrolised at 500°C showed these biochars to be comparatively resistant to degradation. The strong relationships between loss of indigenous carbon from the degraded biochars and amount and $\delta^{13}C$ values of CO_2 efflux in incubation trials led to two main hypotheses which remained unproven: 1. Biochar degradation was predominantly microbial and 2. High local Ca^{2+} concentrations immobilized degradation products in situ at high pH, rather than leaching and loss of degradation products at low pH.

Here we present new evidence of the role of microbial activity in the degradation of the biochar samples previously studied by Bird et al. (2017). We determined the efflux rate of CO_2 in in-vitro incubation experiments and measured both ^{14}C concentration and $\delta^{13}C$ values in the CO_2 efflux with the aim of quantifying the contributions of indigenous radiocarbon-free PyC and exogeneous C sources to CO_2 efflux from degrading biochar. We also tested the hypothesis that high local Ca^{2+} concentrations lead to the immobilization of degradation products on the biochars.

Methods

Biochar samples

Detailed characteristics of the initial biochar material and the field trial was reported by Bird et al. (2014, 2017). In brief, a c. 8 million year old wood log obtained from a brown coal seam was pyrolyzed at 305, 414 or 512 ˚C using the system described by Bird et al. (2011). The radiocarbon contents of the initial biochars were negligible and the TOC content and the proportion of stable polycyclic aromatic carbon (SPAC) at high temperature increased with increasing temperature of pyrolysis (McBeath et al. 2015). As temperature increases, the number of carbon rings increases, leading to the development of recalcitrant microcrystalline graphitic sheets (Preston and Smith 2011). The biochar was used in a 3-year environmental degradation trial at the James Cook University Daintree Rainforest Observatory, Cape Tribulation, Queensland (16.103 °S; 145.447 °E; 70m asl). This site is in a hot (mean monthly temperature ranging from 22 - 28 ˚C) and humid (3,500 mm annual rainfall) rainforest environment, where interactions between biochars and the environment can be expected to be comparatively rapid.

In the field trial, aliquots of each biochar type contained in triplicate 125 µm aperture nylon mesh bags, were pegged to the soil surface from June 2009 to August 2012 and subjected to one of the following four treatments: (i) NL - all litter removed from the surface and aliquots laid directly on the soil surface; (ii) L - as for NL but aliquots then covered with a ~5 cm thick layer of local leaf litter replenished each six months; (iii) NL-LM - as for NL but aliquots then covered with a ~5 cm thick

layer of limestone chips (sieved at 2-10 mm); (iv) L-LM - as for NL but aliquots covered with a layer of limestone chips (sieved at 2-10 mm) mixed with an equal volume of periodically replenished local leaf litter each six months. The purpose of the limestone chips was to increase local pH, as alkaline conditions have been shown to be a significant determinant of PyC degradation behaviour (Braadbaart et al., 2009; Huisman et al., 2012).

Following three years of environmental exposure, Bird et al. (2017) identified correlated increases in ash content (mineral matter after combustion at 550°C), mass of organic carbon, radiocarbon concentration and decrease in $\delta^{13}C$ values in the biochars. The changes were more substantial in 300˚C compared to 500˚C biochars and there were substantial changes in both biochar types according to their physicochemical treatment. The changes were most pronounced in the no-litter (NL) treatments, followed by the changes in the litter (L) treatments while both the no-litter – limestone (NL-LM) and litter – limestone (L-LM) treatments were the least changed after three years.

In vitro incubations and $\delta^{13}C_{CO2}$ and $^{14}C_{CO2}$ measurements

In the present study we conducted two in-vitro experiments to measure the rate and isotopic composition of CO_2 efflux from the field-exposed degraded biochar samples. A small-volume experiment was initially carried out over 66 days to investigate whether there were changes in the rate of CO_2 production and whether changes in C sources may be revealed through changes in the stable isotopic composition of the CO_2 efflux. Subsequently we conducted a second shorter-term (14-18 days) in-vitro experiment to produce larger sample volumes necessary for the measurements of CO_2 ^{14}C concentration.

In the longer-term experiment, aliquots (≈80 mg) of dried 300°C and 500°C biochar (each treatment in duplicate) were placed on a wet pre-combusted quartz sand bed (≈750 mg) in 12 mL capacity Exetainer vials sealed with a septum cap for incubation in the dark at 25 °C over 66 days, with no applied nutrient source. Milli-Q™ grade water, filtered at 0.2 µm and UV-sterilized was added to the surface level of the combusted sand. The wet sand base provided a stable source of moisture available by capillary action without saturating the samples over the course of the experiment. Vials were filled with CO_2-free air immediately after sample loading. No new microbial material was added as the purpose was to measure the response of a reinvigorated microbial population present on the biochars in relation to the labile carbon supply inferred to exist based on the radiocarbon measurements of Bird et al. (2017).

Duplicate samples of the pre-exposure 300 and 500°C biochar and two vials with wet sand only (blanks) were included in the incubation experiment. The volumetric concentration and $\delta^{13}C$ values

of the evolved CO_2 were measured after 1, 4, 7, 11, 18, 30, 38, 49 and 66 days of incubation using a Wavelength-Scanned Cavity Ring-down Spectrometer (Picarro G2131-i). Vial gases were extracted and supplied to the spectrometer via a syringe penetrating the vial septum with simultaneous entry of CO_2-free air through a second syringe. This procedure allowed for the maintenance of sufficient O_2 to support CO_2 production throughout the incubation period. The Picarro G2131-i records CO_2 concentration and $\delta^{13}C$ values at approximately 1 Hz. Integrated CO_2 and $\delta^{13}C$ values over the ≈ 2-5 min analysis time (dependent on CO_2 concentration) were derived using an in-house Excel™ calculation template. The integration window was selected to include all data sets with CO_2 > 40 ppm vol. Calibration of concentration values were carried out by analysis of CO_2-free air and a certified CO_2-in-air standard gas (1050 ppm vol) and $\delta^{13}C$ values were calibrated to the VPDB scale by analysing CO_2 evolved from two in-house carbonate standards ($\delta^{13}C$ = -4.67‰, -24.23‰) tied to the certified reference materials NBS-18 and NBS-19. Precision of the $\delta^{13}C_{CO2}$ measurement is ±1 ‰.

A shorter-term, up-scaled incubation experiment was used to produce larger CO_2 samples for ^{14}C analysis. A 200-1000 mg aliquot (depending on expected reactivity) of each biochar was placed on a ≈10 g pre-combusted wetted quartz sand bed in 300 mL Pyrex flasks, equipped with high vacuum greaseless stopcocks and Viton-O-ring seals, for incubation in the dark at 25°C for 14-18 days. Flask were filled with CO_2-free air immediately after sample loading. Two empty flasks were included as blanks. At the end of the incubation period 12 mL gas samples were extracted from the experimental flasks with a syringe and transferred into Exetainer vials for measurement of $\delta^{13}C$ values as described above. The remaining volume of gas was extracted and CO_2 purified and transferred into sealed quartz tubes using a cryogenic vacuum system. Carbon dioxide samples were graphitised and AMS ^{14}C measurements carried out using the ANTARES facility at the Australian Nuclear Science and Technology Organisation (ANSTO; Fink et al., 2004). Raw measurement results were corrected for possible contamination in graphitisation stage only (Hua et al. 2001). All results are reported as percent modern carbon (pMC) and precision (1σ) ranged from 0.5 - 2.3 pMC (see Bird et al., 2014 for further method details).

Calcium analysis of biochars

To assess the potential transport of calcium from soil, leaf litter and limestone into biochar samples during the 3-year field trial we undertook water and acid extractions of all biochar samples. Aliquots of ≈0.5 g biochar were first extracted in 5 mL of deionised water over a 14-day period. Upon completion, all extracts were mildly to moderately acidic (pH = 4.1- 6.8). The extraction residues were then subjected to a further 24-hour extraction in 5 mL of 5% HNO_3. Calcium concentrations

were analysed by Inductively Coupled Plasma Mass Spectrometry (ICPMS). Analytical quality control included analysis of certified reference waters, replicate samples and spiked samples.

Results

Short-term incubation experiments

The rate of CO_2 efflux was significantly (p=0.002) higher in the 300˚C (13.7 ± 4.5 µmoles/g C/d) compared to the 500˚C biochars (6.1 ± 2.5 µmoles/g C/d) across all treatments in the short-term (14-18 days) incubation experiment (Table 1). There was also a significant (p = 0.018) difference in ^{14}C concentration in CO_2 derived from the two biochars. The lower pMC (percent Modern Carbon) produced from the 300˚C biochar (range 24 - 76, mean 53, n = 8) compared to the 500˚C biochar (range 61 - 87, mean 76, n = 7) across all treatments (Table 1) suggest that less modern C and/or more radiocarbon-dead C is available for conversion to CO_2 in the 300 ˚C biochar compared to the 500 ˚C biochar.

In contrast to CO_2 efflux rate and $^{14}C_{CO2}$ concentration there was no significant (p=0.12) difference in $\delta^{13}C$ -CO_2 values derived from the 300˚C and 500˚C biochars in the short-term incubation experiment. However, $\delta^{13}C$ values varied substantially between treatments, with the lowest $\delta^{13}C$ values (-27 to -30 ‰) recorded in the L and LM (no limestone) treatments of the 300˚C biochar while the highest $\delta^{13}C$ values were measured in the NL-LM and L-LM (with limestone) treatments of both 300˚C and 500˚C biochars (Table 1).

The variation in CO_2 efflux rate and $^{14}C_{CO2}$ concentration in replicate field samples reflects unavoidable differences in the individual field placements including the thickness of covers, ingress of exogenous matter and water as well as rate of microbial colonisation.

Table 1. CO_2 efflux rate and $\delta^{13}C$ values and ^{14}C concentration in CO_2 derived from the short-term (14-18 days) incubation experiment of two biochars (300˚C, 500˚C) each subjected to 4 different physico-chemical treatments during 3 years of environmental exposure (NL: no litter; L: litter; NL-LM: no litter; limestone; L-LM: litter, limestone; field replicates are indicated by appended number). pMC = percent Modern Carbon.

BC ID	Treatment	CO_2 efflux rate (µmoles/g C/d)	$\delta^{13}C$- CO_2 (‰)	ANSTO lab code	$^{14}C_{CO2}$ (pMC)	$^{14}C_{CO2}$ ±1σ error
300	NL-1	20.4	-27	OZU899	75.97	0.75
	NL-2	18.1	-28	OZU900	66.22	0.45
	L-1	15.4	-30	OZU901	64.38	0.43
	L-2	16.3	-27	OZU902	71.61	0.48
	NL-LM-1	10.2	-25	OZU903	26.80	0.27
	NL-LM-2	9.4	-21	OZU904	58.05	0.65
	L-LM-1	11.7	-22	OZU905	36.52	0.29
	L-LM-2	7.8	-20	OZU906	24.00	0.26
500	NL-1	10.0	-25	OZU912	84.95	0.46
	NL-2	6.5	-24	OZU913	74.66	0.82
	L-1	8.3	-25	OZU914	86.87	0.58
	L-2	6.5	-22	OZU915	84.52	0.46
	NL-LM-1	3.4	-21	OZU916	66.82	0.49
	NL-LM-2	3.1	-21	OZU917	61.29	0.76
	L-LM-1*	4.7	-25	OZU918	72.68	0.73

*: Replicate sample L-LM-2 failed AMS analysis

Calcium concentrations in the initial biochar samples before environmental exposure were <10 mg/kg (sum of water and acid extraction, see Supplementary Material File 1). After 3 years of environmental exposure biochars covered with limestone had gained substantially higher amounts of Ca (≈ 300-1200 mg/kg, n=8) than biochars without limestone cover (≈ 115-185 mg/kg, n=8).

Long-term incubation experiments

For the 300˚C biochars, the CO_2 efflux rate peaked at ≈ 18-41 µmoles CO_2/day/g C between day 1 and 4 depending on treatment but slowed to ≈ 1.9-2.5 µmoles CO_2/day/g C by the end of the experiment (day 49-66, see Supplementary Material File 2). Efflux of CO_2 was substantially higher in the two treatments without limestone (NL and L) than in the treatments with limestone (NL-LM and L-LM) (Fig. 1a). Compared to the 300˚C biochars, CO_2 efflux rate and cumulative CO_2 efflux were lower in the 500˚C biochars (initial rate ≈ 6-16 µmoles CO_2/day/g C, final rate ≈ 2.5-3.8 µmoles CO_2/day/g C) but the relative differences between the treatments were similar between the two biochar types (Fig. 1b). The initial biochar sample of both biochar types produced considerably lower CO_2 efflux than the 3-year environmentally exposed samples.

The $\delta^{13}C$ values of CO_2 in the long-term incubation experiment varied over the course of the experiment for most treatments in both biochar types (Fig. 1 c, d). In both 300˚C and 500˚C biochars without limestone (NL and L) $\delta^{13}C$ values were initially low (≈ -27 to -29‰) before rising towards the end of the experiment (≈ -23 to -25‰). In contrast, the $\delta^{13}C_{CO2}$ values in the limestone treatments (NL-LM and L-LM) differed between the two biochar types with the 300˚C biochars stabilizing at higher values (≈ -20 to -23‰) than the 500˚C biochars (≈ -26‰) towards the end of the experiment. While $\delta^{13}C_{CO2}$ values derived from the short-term and long-term incubations varied by 2-3 ‰ at equivalent incubation times the relative difference in values between limestone and no-limestone treatments were similar.

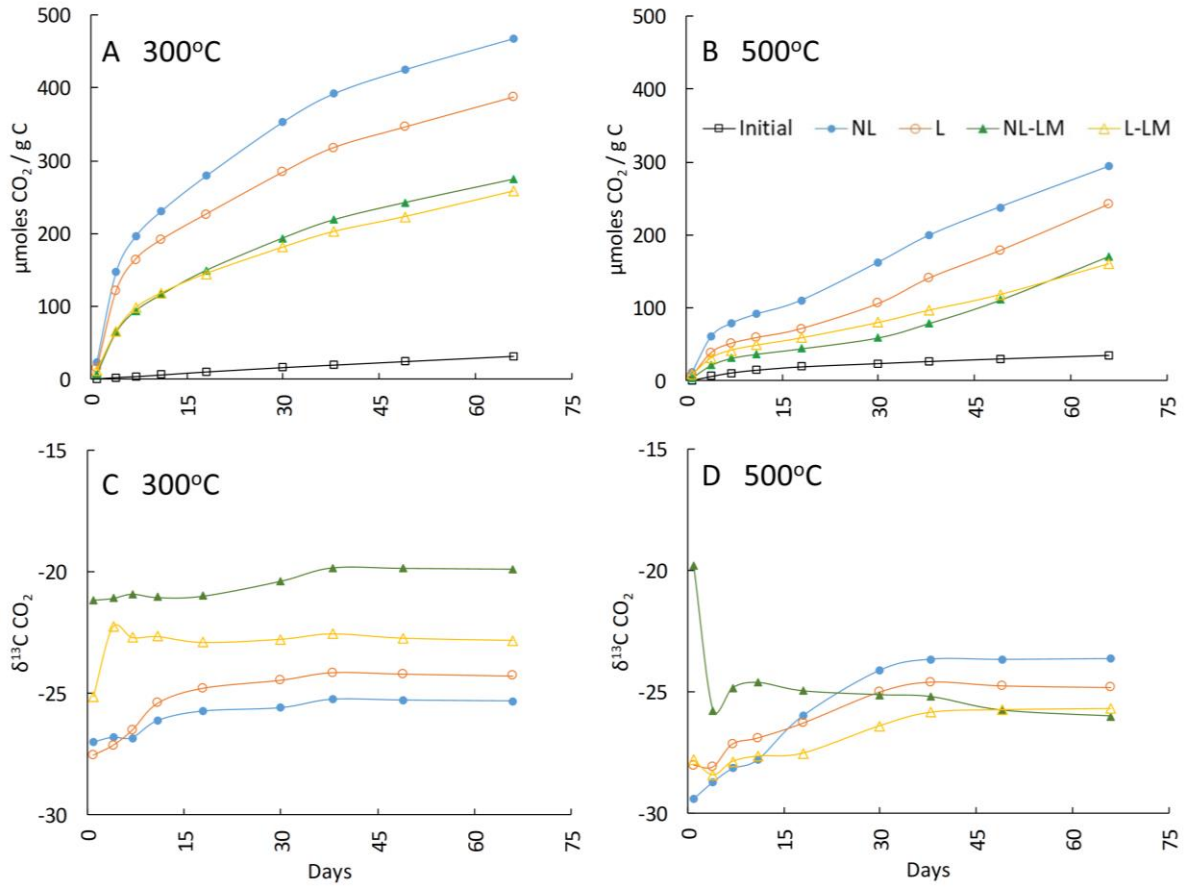

Fig. 1. Cumulative CO_2 efflux (A, B) and $\delta^{13}C_{CO2}$ values (C, D) from 300˚C and 500˚C biochars in 66-day incubation experiments (mean of two replicates of each treatment). CO_2 efflux from the initial samples was insufficient for isotope measurement. NL: no litter cover; L: litter cover; NL-LM: no litter but limestone cover; L-LM: litter and limestone cover.

Discussion:

CO_2 efflux and ^{14}C concentration

Previous studies have used laboratory incubations and ^{14}C labelling to demonstrate that microbial mineralisation and respiration of CO_2 are dominant processes in the degradation of biochar (e.g Singh et al. 2012, Kuzyakov et al. 2014). However, Zimmerman (2010) showed that abiotic oxidation may be a significant degradation process in some cases. In the present study, we use the link between $^{14}C_{CO2}$ concentration and degradation to apportion the measured CO_2 efflux to indigenous biochar C and exogenous C from other sources within the biochars after three years of environmental exposure.

Based on our short-term incubation experiments, we found significant ($p<0.05$) correlations between ^{14}C concentration in both the 300˚C and 500˚C biochars after 3 years of exposure (data from Bird et al. 2017) and the ^{14}C concentration in CO_2 obtained from the incubation experiment (Fig. 2a, note that % ^{14}C-dead C is shown (pDC = 100-pMC) which represents the indigenous C component). The ^{14}C concentration in CO_2 efflux from the 300˚C biochars was also significantly ($p<0.01$) correlated with relative changes in C concentration in these biochars (data from Bird et al. 2017) which is a function of both loss of indigenous C and addition of exogeneous C (Fig. 2b). However, the positive trend between ^{14}C concentration in CO_2 and changes in C concentration in the 500 ˚C biochars was not significant ($p=0.26$).

The ^{14}C pDC values were substantially lower in CO_2 than in the corresponding biochar source material in all treatments of both biochars. Furthermore, there was a higher proportion of indigenous C in CO_2 from 300˚C biochars compared to CO_2 from 500˚C biochars. The limestone treatments of both biochar types had the lowest ^{14}C concentration (highest pDC) in both CO_2 and the biochar source. These findings are consistent with the observations by Bird et al. (2017) that 500˚C biochars are more resistant to decomposition than 300˚C biochars and that biochars treated with limestone had comparatively lower degrees of indigenous carbon loss and lower ingress of exogeneous C compared to treatments without limestone. These authors also hypothesized that restricted oxygen availability and high Ca^{2+} availability were two factors potentially reducing mobility of degraded biochar C and lower ingress of exogeneous carbon in the limestone treatments.

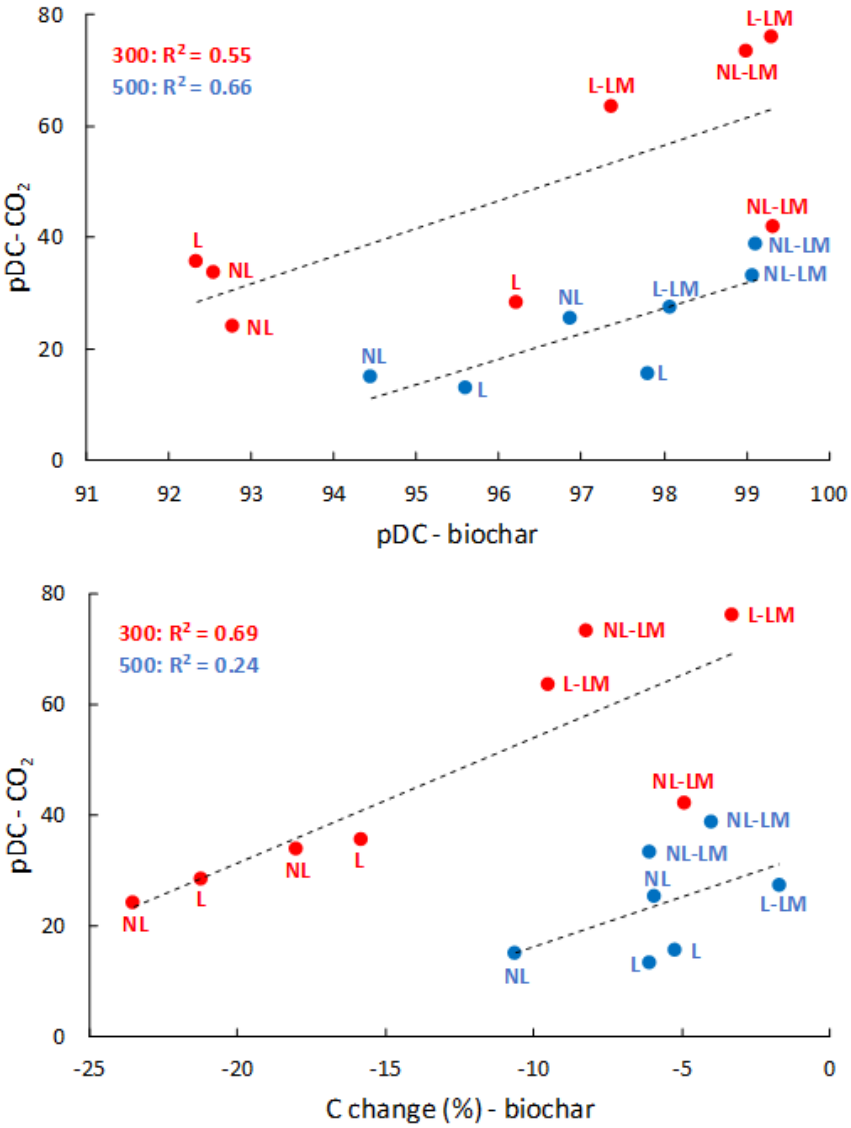

256

257 Fig. 2. Relationship between ^{14}C concentration in CO_2 efflux from biochars (this study) and ^{14}C
258 concentration in biochars and change in biochar C content after environmentally exposure (data
259 from Bird et al. 2017). Radiocarbon concentration is shown as percent ^{14}C-dead carbon (pDC = 100-
260 pMC). NL: no litter cover; L: litter cover; NL-LM: no litter but limestone cover; L-LM: litter and
261 limestone cover. All ^{14}C analytical errors are within the size of the data points shown (maximum
262 error is +/- 0.85 pDC).

263

264 The long-term incubation experiments demonstrated a reduction of up to 20-fold in the CO_2 efflux
265 rate over the duration of the experiment (66 days). In addition, the cumulative $\delta^{13}C_{CO2}$ values of
266 most treatments varied most dramatically over the first approximately 30 days after which time the

values became relatively stable. These observations mean that the ^{14}C and $\delta^{13}C$ data derived from the short-term in-vitro experiment represents an initial phase of rapid CO_2 efflux sourced from a relatively small pool of the most labile C. The reduced efflux of CO_2 in 500˚C biochars compared to 300˚C biochars and in biochars treated with limestone is consistent with an increased content of recalcitrant SPAC in high temperature biochars and an effect of limestone in reducing loss of C. Comparison of the environmentally exposed and initial biochar samples show an ≈ 15-fold increase in the cumulative CO_2 efflux in the 300˚C biochar with no treatment after 66 days. The 500˚C biochars and biochars treated with leaf litter and limestone showed lesser, but still substantial, acceleration in CO_2 efflux from degradation of C.

Biochar degradation and CO_2 sources

Carbon dioxide was derived from two sources of labile C contained in the 3-year old biochars: exogenous C mainly derived from leaf litter with high ^{14}C concentration (pMC ≈106.2, Bird et al. 2014) and a semi-labile fraction of radiocarbon-dead indigenous biochar C (pMC <0.05). The proportional contribution of these two sources can be directly linked to the ^{14}C concentration measured in the CO_2 efflux from the short-term incubation experiment.

Figure 3 shows the changes in composition of biochars over 3 years based on mass balance calculations (based on data from Bird et al. 2017) and the source apportionment of the CO_2 efflux data presented in this study (see Supplementary Material File 3). The mass of inert indigenous C is the measured content of SPAC (McBeath et al. 2015) and is assumed to remain unchanged over the 3-year period. Preservation of indigenous C (blue and orange sections in Figure 3) was highest and ingress of exogenous C (green sections) was lowest in the limestone covered biochars which suggests that biochar degradation was slowed by restricting oxygen availability and ingress by water and microbiota in these treatments. In contrast, the more degraded indigenous C and higher ingress of exogenous C in biochars exposed on the surface, or covered only by leaf litter, was likely caused by higher oxygen availability and increased access for water and microbiota.

The mass balance results and their link to $^{14}C_{CO2}$ concentration demonstrate that a high to dominant proportion (≈ 30-71%) of the CO_2 efflux was derived from the small proportion of exogeneous C (<8 % of total C) in the 300˚C biochars. For the 500˚C biochars, an even higher proportion of CO_2 (≈ 64-86%) was derived from exogeneous C which constituted less than 5 % of total C. Although high proportions of the CO_2 efflux were derived from the small contents of exogeneous C in the biochars,

298 the CO_2 efflux from the incubation experiments accounted for less than 1% of exogeneous C in all
299 samples.

300 The source of the remainder of the CO_2 efflux in both biochar types must be the semi-labile fraction
301 of indigenous C which amounts to ≈25-56% of the total biochar mass in the 300˚C biochar and ≈22-
302 28% of the total biochar mass in the 500˚C biochars (depending on treatment). Depending on
303 treatment, respiration rates of indigenous biochar carbon amounted to ≈ 0.7 - 1.4 µmoles CO_2 / g C /
304 day for the 300˚C biochar and 0.5 - 1.3 µmoles CO_2 / g C / day for the 500˚C biochar at the end of the
305 long-term incubation experiment (Supplementary Material File 4). It is interesting to note that at
306 these respiration rates the indigenous carbon pool would be completely degraded in ≈230-650
307 years.

308 The CO_2 efflux rates obtained for both the 300˚C and 500˚C biochars as a proportion of the semi-
309 labile indigenous PyC component were up to twice the maximum abiotic rate of degradation of
310 biochars reported by Zimmerman (2010) and other studies have documented their high resistance
311 to chemical oxidants (Forbes et al. 2006, Wang et al. 2016). Since the only oxidizing agents available
312 in our biochar incubations were the initial volume of deionised water and air, it seems improbable
313 that abiotic oxidation and/or solubilisation could be the dominant degradation processes.
314 Consequently, we infer that most of the CO_2 produced over the course of the incubations was due to
315 microbial degradation and respiration. However, abiotic oxidation may become increasingly
316 important in longer term incubations upon exhaustion of the most microbially available C sources.

317

318

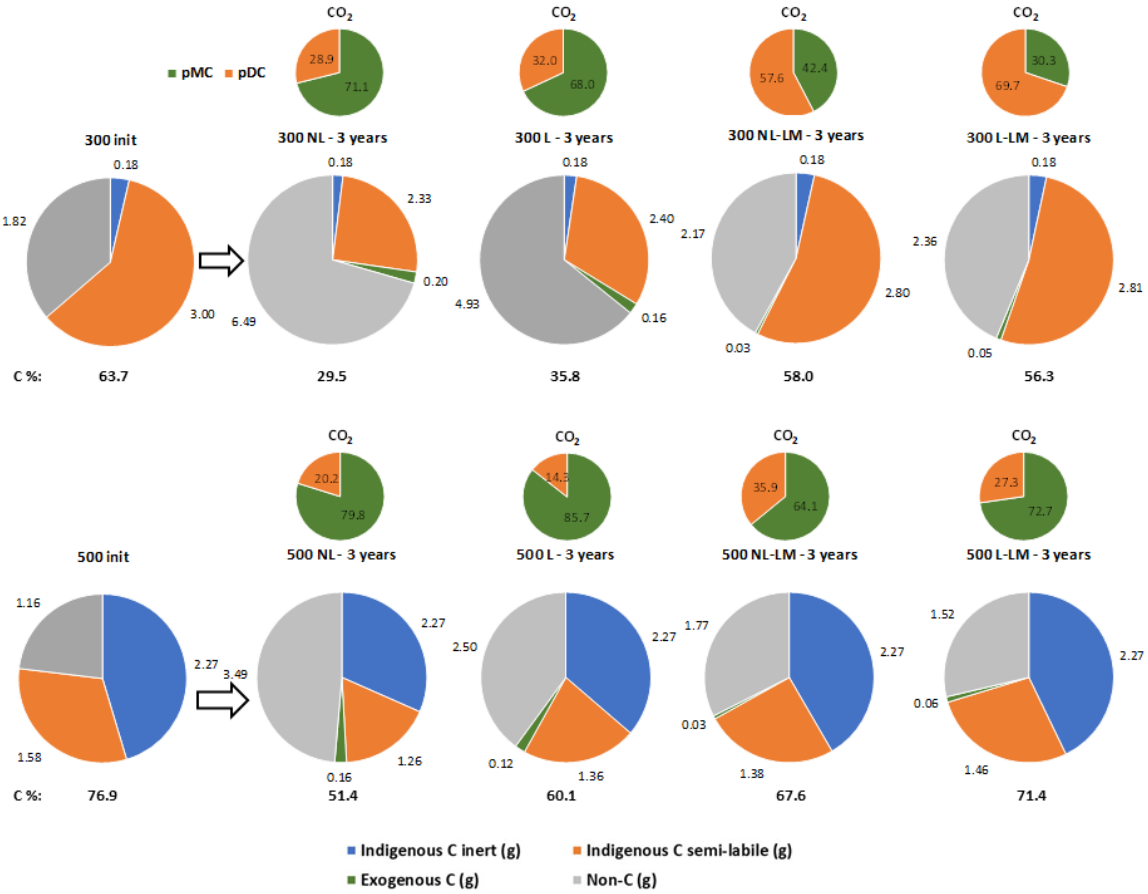

319

320 Fig. 3. Depiction of the distribution of carbon and non-carbon components in biochars before and
321 after environmental exposure (large pie-charts) based on biochar mass balance data from Bird et al.
322 (2017) and CO_2 efflux data from the present study. The mass (g) of each component is indicated
323 outside each pie chart (initial biochar mass = 5 g) and the C concentration (%) is shown below. The
324 small pie-charts show % modern carbon (pMC) and ^{14}C-dead carbon (pDC) in the CO_2 efflux from
325 exogeneous and indigenous semi-labile C, respectively. NL: no litter cover; L: litter cover; NL-LM: no
326 litter but limestone cover; L-LM: litter and limestone cover.

327

328 A two-component mixture of CO_2 efflux from the indigenous and exogenous C sources identified can
329 account for the distribution of both $\delta^{13}C$ and ^{14}C pMC values in most of biochar samples (Fig. 4).
330 Carbon dioxide derived from both indigenous C (biochar <0.05 pMC, Bird et al. 2014) and exogenous
331 C (leaf litter = 106.2 pMC, Bird et al. 2014) is likely to have a range of $\delta^{13}C$ values close to those of
332 the C source itself (300˚C biochar initial $\delta^{13}C$ = -20.7‰, 500˚C biochar initial $\delta^{13}C$ = -21.0‰, forest
333 litter $\delta^{13}C$ = -29.0‰, Bird et al. 2014). In a study of Australian grasslands, Šantrůčková et al. (2000)
334 found that the $\delta^{13}C$ value of microbial C on average was enriched by ≈2‰ compared to soil organic
335 C, while microbially-respired CO_2 on average had $\delta^{13}C$ values depleted by ≈ 2.2‰ compared with

microbial C. Assuming that similar isotopic fractionation effects occurred in the in-vitro respiration of our biochar samples, a $\delta^{13}C_{CO2}$ value of -2.2‰ below the initial source C (both indigenous C and exogenous leaf litter C) would result from the direct respiration of these two C sources. In addition, an upper $\delta^{13}C_{CO2}$ value of 2‰ above the initial source C would result from the in-vitro respiration of CO_2 by microbes obtaining C from dead microbial matter contained in the biochars and which obtained C from the indigenous and/or exogenous C sources during the 3 -year environmental exposure of the biochar. Figure 4 demonstrates that the main influence on ^{14}C concentration and $\delta^{13}C$ values in CO_2 efflux from the degrading biochars was the limestone treatment and not the biochar type (300°C or 500°C).

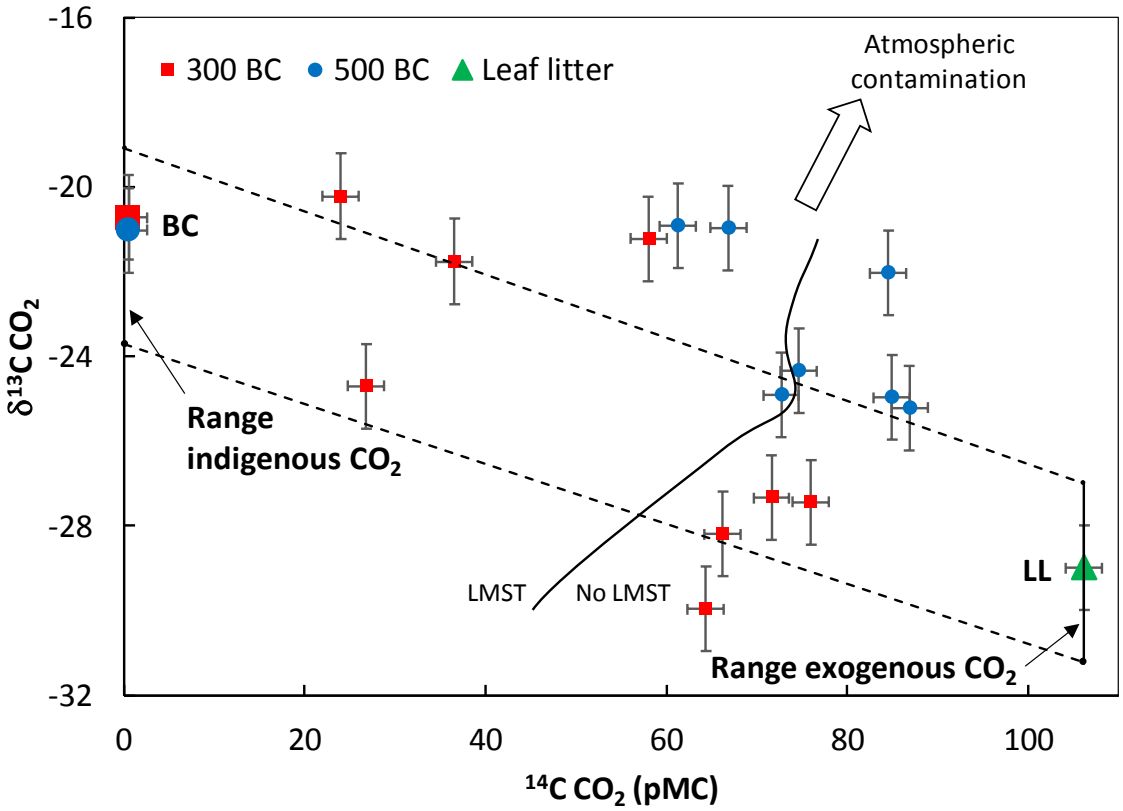

Fig. 4. Relationship between $\delta^{13}C$ values and ^{14}C concentrations (pMC) in CO_2 efflux from environmentally exposed biochars in short-term (14-18 day) incubation experiments. The range of likely values in CO_2 respired from the initial indigenous (biochar 'BC') and exogenous (leaf litter 'LL') sources are based on data from Bird et al. (2014) and Šantrůčková et al. (2000). The broken lines represent mixing between indigenous and exogenous C sources. The full line distinguishes limestone

353 treatments (LMST). The wide arrow indicates displacement of samples due to possible air
354 contamination during sample preparation.

355

356 The $\delta^{13}C_{CO2}$ values of four samples were approximately 2-3‰ higher than expected from mixing of
357 the indigenous and exogenous CO_2 sources. We considered the possibility that three of these higher
358 $\delta^{13}C$ values (samples with limestone treatment) could be due to incorporation of carbonate
359 fragments. However, the acidic nature of the biochars (pH = 4.5 to 5.6, Bird et al. 2017) would tend
360 to rapidly dissolve carbonates. In addition, we found no association between $\delta^{13}C_{CO2}$ values and Ca
361 concentrations in water extracts of the 300˚C or 500˚C biochars (Fig. 5). This suggests that there was
362 no limestone present in the biochar samples that could contribute CO_2 with high $\delta^{13}C$ values.
363 Therefore, the elevated Ca concentrations in biochars covered with limestone must indicate that
364 Ca^{2+} ions were derived by dissolution of the overlying limestone and immobilised within the
365 biochars. The small increase in Ca content in biochars without limestone treatment relative to the
366 initial biochar content likely indicates a lesser influx of Ca from local surface soils (exchangeable Ca ≈
367 1,600 mg/kg, unpublished data). As we have not identified any other source of CO_2 with high $\delta^{13}C$
368 values within the biochar samples it seems likely that the four samples with $\delta^{13}C$ values above the
369 upper mixing line in Fig. 4 were contaminated with atmospheric air ($\delta^{13}C \approx -7.5$ ‰), possibly due to
370 incomplete flushing of the incubation flasks with CO_2 free air, a scenario considered likely given the
371 small sample sizes (average 47 µg C). An isotopic mass balance calculation shows that a maximum of
372 12% of atmospheric air would account for the displacement of all samples above the upper mixing
373 line in Fig. 4.

374

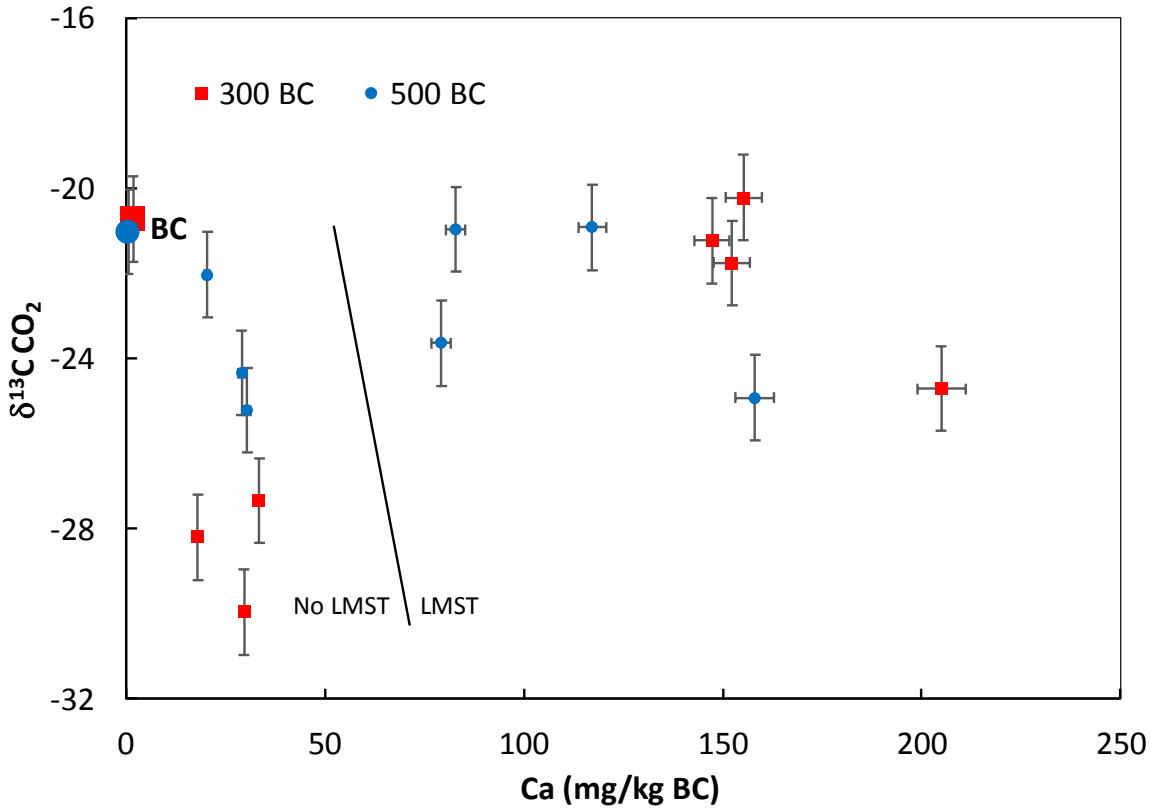

Fig. 5. Relationship between $\delta^{13}C_{CO2}$ values and Ca concentrations in water extractions of environmentally exposed biochars. The full line distinguishes limestone treatments (LMST) and 'BC' indicates the likely values in CO_2 respired from the initial biochar samples (data from Bird et al. 2014).

Influence of Ca^{2+} availability on biochar degradation

The observation that CO_2 respired from the limestone-treated biochars contained substantially more radiocarbon-dead indigenous C (lower pMC values), and that those incubations contained more Ca, compared to biochars without limestone treatment, supports the hypothesis by Bird et al (2017) that the availability of Ca^{2+} ions reduces the mobility of degraded indigenous biochar. In addition, the limestone covers restricted access by oxygen, water and microbiota. Table 2 shows the calculated losses of indigenous C respired as CO_2 as a percentage of the total indigenous C loss over the 3-year field trial. The calculations are based on the respiration rates measured during the final 17 days of the 66-day incubation trial (see Supplementary Material File 4). Irrespective of whether these rates accurately reflect field conditions during environmental exposure the data illustrates the effect of limestone treatment in reducing the field mobility of degraded indigenous C in biochars.

Limestone treated 300˚C biochars had a 5-6 fold higher percentage indigenous C loss respired as CO_2 compared to treatments without limestone. In the 500˚C biochars the increase was 2-3 fold. The lower percentages in the 300˚C compared to the 500˚C biochars are due to the larger pool of semi-labile indigenous C available for respiration in the 300˚C biochars (94% of total indigenous C) compared to the 500˚C biochars (41% of total indigenous C). The results here suggest higher Ca^{2+} availability led to the binding and immobilization *in situ*, of degradation products to the char surfaces, or minerals associated with the char surfaces (Oades, 1988; Wittinghall and Hobbie, 2012; Varcoe et al., 2010).

The difference in respired loss of indigenous C between limestone and no limestone treatments indicates the amount of additional loss by solubilisations and leaching of indigenous C in biochars without limestone treatment. While all biochars, regardless of treatment type, were degraded during the period of environmental exposure, a significant portion of the resulting labile C was not leached from the biochars treated with limestone. Hence a larger pool of indigenous carbon was available for respiration in the laboratory incubations as shown in Fig. 3.

Table 2. Calculated indigenous C respired as CO_2 as a percentage of the total indigenous C loss during the 3-year field trial

	No litter No Limestone	Litter No limestone	No litter Limestone	Litter Limestone
300 ^{o}C biochar	4.5%	5.4%	21.9%	30.4%
500 ^{o}C biochar	10.5%	12.6%	32.7%	28.4%

The finding that Ca^{2+} availability has an impact on the immobilization of degradation products on biochars has implications for the radiocarbon dating of ancient biochars. Biochars from alkaline environments appear more degraded than samples from non-alkaline environments (Alon et al., 2002; Rebollo et al., 2008). The results presented here suggest that biochars from alkaline environments are not intrinsically more susceptible to degradation than biochars from non-alkaline environments, they simply retain degradation products in situ through Ca^{2+} immobilization processes – products that have been lost by leaching and/or respiration from chars in non-alkaline environments. Thus, the often-large alkali-soluble component of ancient biochars from Ca-rich

environments such as limestone caves may be of mostly indigenous origin. As such the alkali-soluble component may potentially be able to provide a robust radiocarbon age determination if the solubilized indigenous component can be isolated from actual exogenous contamination.

Conclusions:

We have reported ^{14}C concentration and $\delta^{13}C$ values of the CO_2 efflux from incubated biochars previously degraded during 3 years of environmental exposure in a humid tropical environment. The radiocarbon results show that one degradation pathway, likely mediated by microbial activity, lead to the respiration of indigenous biochar carbon in significant amounts as CO_2 along with a component of exogenous carbon closely associated with the biochars but derived from the local environment. In addition, correlations observed between ^{14}C concentration, $\delta^{13}C$ values and Ca abundance indicate that high Ca^{2+} availability reduces loss of indigenous C during biochar degradation by immobilizing degradation products in-situ.

Acknowledgements: The authors acknowledge the ANSTO CAS radiocarbon chemistry team for the processing of the sample carbon dioxide break seals into graphite accelerator targets.

Funding:

This project was supported by an Australian Research Council Laureate Fellowship (FL140100044) to MIB and ANSTO Portal Grant PE10105 to MIB and VAL. VAL and AW acknowledge the financial support from the Australian Government for the Centre for Accelerator Science at ANSTO, where the ^{14}C measurements were done, through the National Collaborative Research Infrastructure Strategy.

References:

Alon D, Mintz G, Cohen I, Weiner S, Boaretto, E 2002. The use of Raman spectroscopy to monitor the removal of humic substances from charcoal: quality control for 14C dating of charcoal. *Radiocarbon* 44(1): 1-11.

Bird MI, Ayliffe LK, Fifield K, Cresswell R, Turney C 1999. Radiocarbon dating of 'old' charcoal using a wet oxidation - stepped combustion procedure. *Radiocarbon* 41(2): 127-140.

449 Bird, MI, Wurster CW, de Paula Silva PH, Bass A, de Nys R 2011. Algal biochar production and
450 properties. *Bioresource Technology* 102: 1886-1891.

451 Bird MI 2013. Charcoal. In: Elias S.A. (ed.) *The Encyclopedia of Quaternary Science* (2nd edition), Vol. 4
452 pp. 353-360. Amsterdam: Elsevier.

453 Bird MI, Levchenko V, Ascough PL, Meredith W, Wurster CM, Williams A, Tilston EL, Snape CE,
454 Apperley DC 2014. The efficiency of charcoal decontamination for radiocarbon dating by three pre-
455 treatments–ABOX, ABA and hypy. *Quaternary Geochronology* 22: 25-32.

456 Bird MI, Wynn JG, Saiz G, Wurster CM, McBeath A 2015. The pyrogenic carbon cycle. *Annual Reviews*
457 *of Earth Planetary Sciences* 43: 273–298.

458 Bird MI, McBeath AV, Ascough PL, Levchenko VA, Wurster CM, Munksgaard NC, Smernik RJ, Williams
459 A. 2017. Loss and gain of carbon during char degradation. *Soil Biology & Biochemistry* 106: 80-89.

460 Braadbaart F, Poole I, Van Brussel AA 2014. Preservation potential of charcoal in alkaline
461 environments: an experimental approach and implications for the archaeological record. *Journal of*
462 *Archaeological Science* 368: 1672-1679.

463 Fang Y, Singh B, Singh BP, Krull E 2014. Biochar carbon stability in four contrasting soils. *European*
464 *Journal of Soil Science* 65: 60–71.

465 Fink D, Hotchkis M, Hua Q, Jacobsen G, Smith AM, Zoppi U, Child D, Mifsud C, van der Gaast H,
466 Williams A, Williams M 2004. The ANTARES AMS facility at ANSTO. *Nuclear Instruments and Methods*
467 *in Physics Research Sect. B* 224: 109–115. DOI: 10.1016/j.nimb.2004.04.025.

468 Forbes MS, Raison RJ, Skjemstad JO. Formation, transformation and transport of black carbon
469 (charcoal) in terrestrial and aquatic ecosystems. *Science of the Total Environment* 370: 190–206.

470 Hammes K, Torn MS, Lapenas AG, Schmid MWI. 2008. Centennial black carbon turnover observed in
471 a Russian steppe soil. *Biogeosciences* 5: 1339–1350.

472 Hockaday WC, Grannas AM, Kim S, Hatcher PG. 2007. The transformation and mobility of charcoal in
473 a fire-impacted watershed. *Geochimica et Cosmochimica Acta* 71: 3432–3445.

474 Hua Q, Jacobsen GE, Zoppi U, Lawson EM, Williams AA, Smith AM, McCann MJ 2001. Progress in
475 radiocarbon target preparation at the ANTARES AMS centre. *Radiocarbon* 43 (2A): 275-282.

476 Huisman, DJ, Braadbaart F, van Wijk IM; van Os BJH 2012. Ashes to ashes, charcoal to dust:
477 micromorphological evidence for ash-induced disintegration of charcoal in Early Neolithic LBK soil
478 features in Elsloo The Netherlands. *Journal of Archaeological Science* 394: 994-1004.

479 Kanaly RA, Harayama S. 2000. Biodegradation of high-molecular-weight polycyclic aromatic
480 hydrocarbons by bacteria. *Journal of Bacteriology* 182: 2059–2067.

481 Kuzyakov Y, Bogomolova I, Glaser B 2014. Biochar stability in soil: Decomposition during eight years
482 and transformation as assessed by compound-specific ^{14}C analysis. *Soil Biology and Biochemistry* 70:
483 229-236.

484 McBeath AV, Wurster CM, Bird MI 2015. Influence of feedstock properties and pyrolysis conditions
485 on biochar carbon stability as determined by hydrogen pyrolysis. *Biomass and Bioenergy* 73: 155-
486 173.

487 Oades JM 1988. The retention of organic matter in soils. *Biogeochemistry 5*(1): 35-70.

488 Pietikäinen J, Kiikkilä O, Fritze H 2000. Charcoal as a habitat for microbes and its effect on the
489 microbial community of the underlying humus. *Oikos* 89:231–242.

490 Rebollo NR, Cohen-Ofri I, Popovitz-Biro R, Bar-Yosef O, Meignen L, Goldberg P, ... & Boaretto E 2008.
491 Structural characterization of charcoal exposed to high and low pH: implications for ^{14}C sample
492 preparation and charcoal preservation. *Radiocarbon* 50(2): 289-307.

493 Šantrůčková H, Bird MI, Lloyd J 2000. Microbial processes and carbon-isotope fractionation in
494 tropical and temperate grassland soils. *Functional Ecology* 14(1): 108-114.

495 Singh BP, Cowie AL, Smernik RJ 2012. Biochar carbon stability in a clayey soil as a function of
496 feedstock and pyrolysis temperature. *Environmental Science and Technology* 46: 11770−11778.

497 Varcoe J, van Leeuwen JA, Chittleborough DJ, Cox JW, Smernik RJ, Heitz A 2010. Changes in water
498 quality following gypsum application to catchment soils of the Mount Lofty Ranges, South Australia.
499 *Organic Geochemistry* 41(2): 116-123.

500 Wang J, Xiong Z, Kuzyakov Y 2016. Biochar stability in soil: meta-analysis of decomposition and
501 priming effects. Global Change Biology Bioenergy 8: 512-523.

502 Whittinghill KA, Hobbie SE 2012. Effects of pH and calcium on soil organic matter dynamics in
503 Alaskan tundra. *Biogeochemistry* 111(1-3): 569-581.

504 Woolf D, Amonette JE, Street-Perrott FA, Lehmann J, Joseph S 2010. Sustainable biochar to mitigate
505 global climate change. *Nature Communications* 1:56. DOI: 10.1038/ncomms1053.

506 Zimmerman AR 2010. Abiotic and microbial oxidation of laboratory-produced black carbon biochar.
507 *Environmental Science and Technology* 444: 1295-1301.